Earth and Planetary Science Letters 298 (2010) 66–76

Contents lists available at ScienceDirect

Earth and Planetary Science Letters

journal homepage: www.elsevier.com/locate/epsl

Paleomagnetism of impact spherules from Lonar crater, India and a test for impact-generated fields

Benjamin P. Weiss [a,*], Shelsea Pedersen [a], Ian Garrick-Bethell [a,1], Sarah T. Stewart [b], Karin L. Louzada [b], Adam C. Maloof [c], Nicholas L. Swanson-Hysell [c]

[a] Department of Earth, Atmospheric, and Planetary Sciences, Massachusetts Institute of Technology 54-814, 77 Massachusetts Ave., Cambridge, MA 02139, United States
[b] Department of Earth and Planetary Sciences, Harvard University, 20 Oxford Street, Cambridge, MA 02138, United States
[c] Department of Geosciences, Princeton University, Princeton, NJ 08544, United States

ARTICLE INFO

Article history:
Received 25 May 2010
Received in revised form 2 July 2010
Accepted 8 July 2010
Available online 17 August 2010

Edited by: L. Stixrude

Keywords:
impact craters
Lonar crater
paleomagnetism
spherules
melt rocks
paleointensity
impact-generated fields
Moon
Mars
asteroids

ABSTRACT

Planetary surfaces have been ubiquitously melted by meteoroid impacts throughout solar system history. The resulting impact melts form some of the youngest igneous samples from rocky bodies like the Moon, Mars, and asteroids. Upon cooling, these melts may record any ambient planetary magnetic fields as well as postulated transient fields generated by impact plasmas. Impact-generated fields have been proposed as a key alternative to the core dynamo hypothesis for the paleomagnetism of extraterrestrial bodies. Here we describe a paleomagnetic study of basaltic impact glasses from the Lonar impact crater situated in the Deccan Traps in Maharashtra, India. Previous theoretical work predicts extremely strong magnetic fields (possibly >1,000 times the Earth's surface field) may have been transiently generated during the Lonar impact. We find that the glasses contain a natural remanent magnetization (NRM) whose properties depend strikingly on sample mass. Small (<0.5 g), splash-form samples demagnetize erratically and are inefficiently magnetized, while larger, irregularly shaped samples contain a stable component that is efficiently magnetized similar to Lonar basalts. However, the rock magnetic recording properties of these samples are uncorrelated with mass. Therefore, we conclude that the size dependence of the NRM reflects a difference in how the samples acquired thermoremanence. The splash forms of the smaller samples indicate they cooled during flight and therefore that they were magnetized while in motion, explaining their weak and unstable NRM. This motional NRM is a new manifestation of thermoremanent magnetization not observed before in geologic samples. No glasses contain evidence for any strong (>~100 μT) impact-generated fields.

1. Introduction

The evolution of magnetic fields on the terrestrial planets and in interplanetary space is unknown for most of solar system history. A key limitation is that igneous and sedimentary rock records on the terrestrial planets other than Venus largely predate 3 billion years (Ga) ago. An exception is the volumetrically small but nearly ubiquitous melt that has been continuously created by hypervelocity impacts over nearly all of solar system history. The most abundant and diverse recent such samples in the lunar and meteoritic sample suite are in the form of quickly cooled glass spherules, glassy agglutinates, melt breccias, and macroscopic melt rocks (Chao et al., 1970; Hartung et al., 1978; Rubin, 1985). In particular, recent analyses of lunar regolith have identified hundreds of impact and volcanic glass spherules and fragments per gram of regolith with $^{40}Ar/^{39}Ar$ ages ranging from 4 Ga to the present (Culler et al., 2000; Levine et al., 2005; Zellner et al., 2009a, b). Their counterparts on Earth are crater-associated impact glasses, tektites strewn fields, and spherule layers in ancient sediments (Dressler and Reimold, 2001; Koeberl, 1986; Lowe and Byerly, 2010; Simonson and Glass, 2004).

Nearly all rocks previously analyzed by paleomagnetic methods were stationary when they were magnetized. However, small impact spherules cool during flight and so are not stationary while they are exposed to planetary magnetic fields. As a result, their magnetic records may have affinities to explosive volcanic materials (e.g., spherules and ashes), cosmic spherules, and chondrules and refractory inclusions in chondritic meteorites. Whereas impact melts sample relatively recent planetary history, chondrules and refractory inclusions are the main rock record of the preaccretional epoch of the solar system. Therefore, understanding how impact spherules become magnetized and characterizing the fidelity of their paleointensity records is of great importance for the study of extraterrestrial paleomagnetism.

Impact spherules also offer another unusual but important opportunity. Paleomagnetic analyses of about a dozen young (<3 Ga

* Corresponding author. Tel.: +1 617 324 0224; fax: +1 617 253 8298.
E-mail address: bpweiss@mit.edu (B.P. Weiss).
[1] Now at Department of Geological Sciences, Brown University, Box 1836, Providence, RI, 02912.

0012-821X/$ – see front matter © 2010 Elsevier B.V. All rights reserved.
doi:10.1016/j.epsl.2010.07.028

old) lunar impactites have suggested the surprising result that there were substantial fields (~1 μT) on the Moon within the last few hundred million years (Fuller and Cisowski, 1987). Because it is unlikely that there was a dynamo on the Moon this recently, it has been suggested that this paleomagnetism is the product of transient, impact-generated or amplified fields (via current generation in the conducting plasma cloud) (Crawford and Schultz, 1999). The possibility that impacts can briefly generate magnetic fields can be tested by studying the paleomagnetism of quickly cooled impactites like spherules from well-constrained geologic settings on Earth.

A straightforward way to search for impact-generated fields and to assess whether impact glasses are suitable for paleointensity measurements is to study fresh impactites from young, terrestrial impact craters. With this goal, during field trips in 2005 and 2006 we collected thousands of samples of basaltic glass from the perimeter of Lonar crater, a 1.8-km-diameter impact crater which formed approximately 50,000 years ago in the Deccan Traps in Maharashtra, India [see (Maloof et al., 2010) and references therein]. A theoretical investigation (Crawford and Schultz, 1999) suggested that impact-related fields with intensities ranging up to ~0.1 T (more than 1,000 times the Earth's present surface field) at 1 crater radius distance and lasting for ~1 s could have been produced by the impactor that formed a Lonar-sized crater (assuming the bolide had a ~35 m radius, 2800 kg m^{-3} density, and impact velocity of 20 km^{-1}). This investigation is part of a multidisciplinary study of the structural geology (Maloof et al., 2010) and paleomagnetism (Louzada et al., 2008) of what is the only fresh impact crater on the Earth entirely and unequivocally in a continental basaltic target. As such, Lonar is a unique terrestrial analog for the large number of craters in basaltic terranes on the surfaces of the Moon, Mars, and Venus.

2. Lonar impact glasses

We collected basaltic impact glass (Nayak, 1972; Fredriksson et al., 1973a, 1973b; Sengupta, 1986; Murali et al., 1987; Osae et al., 2005; Ghosh and Day, 2009; Misra et al., 2009) using nonmagnetic tools and sample handling techniques from six localities situated several hundred meters to the east, west and north of the crater rim (for details on sampling locations, see Fig. 4 of Maloof et al., 2010). The smaller glasses (<0.5–0.8 g and <3 mm in radius) primarily have splash forms: they have rounded habits indicating that they are fläden and impact spherules formed from molten ejecta that cooled in mid-air while subject to rotational and aerodynamic forces (Fig. 1) (for a theoretical explanation of impact melt forms, see Elkins-Tanton et al., 2003). Essentially all larger glasses (with masses ~>0.5–0.8 g and ~>3 mm in radius) have irregular but partially rounded shapes, indicating they may have been still partially molten after landing (Fig. 1). The largest of such samples analyzed here are actually a mixture of glass and vesicular, fine grained impact melt. There are some glasses with irregular rounded shapes smaller than 0.5 g, but nearly all such glasses have angular faces, indicating they were once part of larger objects which fractured following solidification. We also found large (up to ~20 cm in diameter), irregular frothy black glasses on the east rim and the "Little Lonar" depression that show little evidence for aerodynamic sculpting.

Previous studies have found that Lonar spherules contain schlieren, relic microlites, and a major element composition very similar to the local Deccan basalt (and with little volatile element depletion) (Fredriksson et al., 1973a; Misra et al., 2009; Osae et al., 2005; Son and Koeberl, 2007). These data collectively indicate that the glasses are direct melts of the local Deccan Trap basalt rather than condensates from an impact-generated vapor plume (e.g., Warren, 2008).

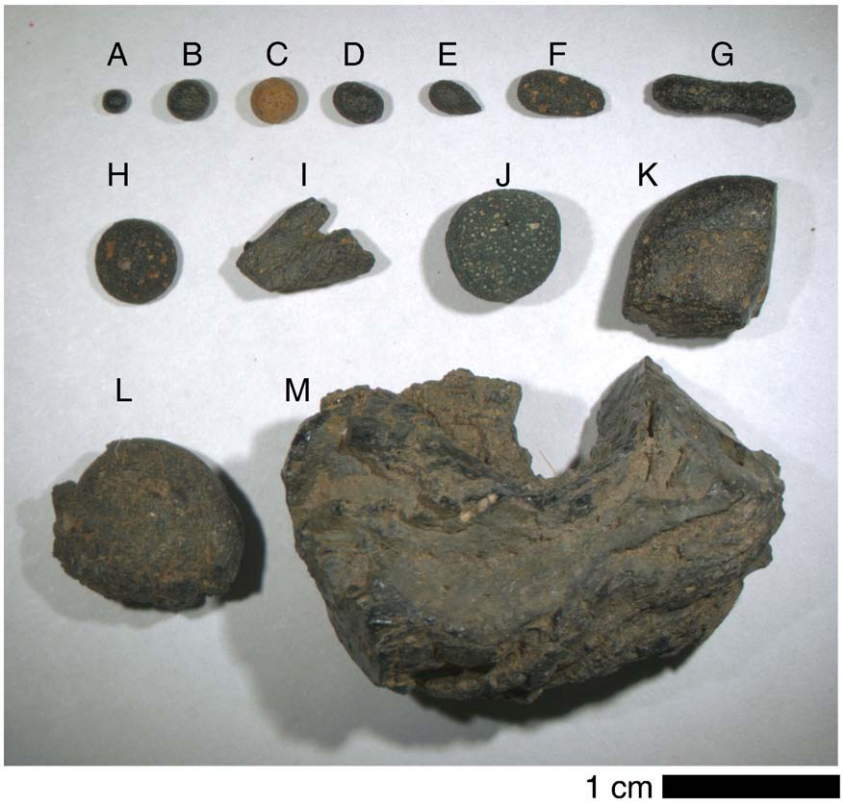

Fig. 1. Basaltic impact glasses recovered from the west rim of Lonar Crater, India. Masses ranged from mg (A) to g (M). (A–H, J) Small glasses showing splash forms including spheres, ellipsoids, teardrops, half-dumbbells, and dumbbells. Most glasses (A-B, D-M) found lying on the surface had glassy interiors and occasional patches of thin (<0.2 mm thick) orange (presumably lepidocrocite) weathering rinds. Heavily weathered spherules (C) were found buried several centimeters beneath the surface. Nearly all glasses larger than ~0.7 g (K–M) have irregular non-splash forms. Most smaller glasses that do not exhibit splash forms have fractured surfaces (I), indicating they were one part of larger, solidified glasses.

Here we present paleomagnetic analyses on 65 splash-form glass spherules and large irregular glassy samples with masses ranging from <0.01 mg to 4.3 g (diameters<100 μm to several cm). Following the categorization of Osae et al. (2005), most of these glasses are apparently of type "a" (glassy splash form), while some of the largest samples grade into types "b" or "c" (clast-rich melt or melt rock). All but the five smallest of these samples were found on the west rim (see Fig. 4 of Maloof et al., 2010). The remaining five were tiny (<0.5 mm diameter) glass spherules (estimated masses ranging from<0.01 to~0.5 mg) discovered near the southeast rim from the same locality (within ~3 m) as the spherules studied by Misra et al. (2009) (see Fig. 4 of Maloof et al., 2010).

Paleomagnetic and rock magnetic remanence data were acquired in the MIT Paleomagnetism Laboratory with a 2G Enterprises Superconducting Rock Magnetometer 755 using an automated sample handling system (Kirschvink et al., 2008). Individual glasses were subject to progressive alternating field (AF) and/or thermal demagnetization. Some samples were only AF demagnetized (to peak fields ranging from 10 to 290 mT depending on the observed NRM stability), while other samples were first AF demagnetized to peak fields of 10 mT [to remove any isothermal remanent magnetization (IRM) overprints from sample handling] followed by thermal demagnetization up to somewhere between 500 and 650 °C. Following NRM demagnetization, most samples also were analyzed using progressive IRM and anhysteretic remanent magnetization (ARM) acquisition followed by AF demagnetization (following Cisowski, 1981). Selected samples were also characterized with room-temperature hysteresis loops acquired with a Digital Measurement Systems vibrating sample magnetometer in the laboratory of C. Ross in the MIT Department of Materials Science and Engineering.

3. Natural remanent magnetization

We found that all samples carry an NRM. However, the samples exhibited one of two classes of behaviors during demagnetization that correlates with their masses. Large (~>0.8 g) samples, which were irregularly shaped, exhibit one or more low blocking temperature and low coercivity magnetization components and a high blocking temperature component stable to between 420 and 540 °C (Fig. 2A, B, F). Thermal demagnetization to these temperatures reduced the NRM intensity to 0.48% (1 standard deviation, $1\sigma = 0.42\%$ for number of samples, $N = 10$) of its initial value on average (Fig. 3A, Table S1). Our least squares fits using principal component analysis (Kirschvink, 1980) to the high temperature and/or high coercivity magnetization identified origin-trending, linear components with maximum angular deviation (MAD) values of 1.4° on average ($1\sigma = 0.4°$, $N = 8$) (Fig. 3B, Table S1).

We found that our small (<~0.5 g) samples, all of which had splash forms, had far smaller NRM per unit mass than large samples (Fig. 4A, Table S1). During demagnetization, sometimes a stable low blocking temperature (100–300 °C) and low coercivity component (10 mT or less) was removed. This is likely viscous remanent magnetization from the Earth's field, which should remagnetize magnetite crystals with 1-h blocking temperatures of ~140 °C over the last ~50,000 years since crater formation (e.g., Pullaiah et al., 1975). However, following this mild heating or AF demagnetization, the small spherule NRM directions exhibited large (typically tens of degree) changes in direction with little decrease in moment intensity (Fig. 2C, D, E). Thermal demagnetization to between 200 and 690 °C and AF demagnetization to >85 mT only reduced the NRM intensity of the small samples to 76% of their initial values on average ($1\sigma = 114\%$, $N = 43$) (Fig. 3A, Table S1). The high temperature and high coercivity magnetization directions are scattered and do not define linear components, such that least squares fits have MAD values on average of 27° ($1\sigma = 12°$, $N = 43$) (Fig. 3B, Table S1).

For basaltic glasses and rocks that have acquired a single-component TRM, the ratio of NRM to saturation isothermal remanent magnetization (sIRM) is roughly proportional to the intensity of the field which magnetized a sample, with a ratio of ~1.5% indicative of an Earth-strength (several tens of μT) field (Gattacceca and Rochette, 2004; Kletetschka et al., 2004; Yu, 2006). The measured NRM/sIRM values for the small samples range have an average value of 0.19% ($1\sigma = 0.14\%$, $N = 45$), while the large samples have ratios on average more than 5 times larger (1.2%; $1\sigma = 0.7\%$, $N = 9$) (Fig. 3C, Table S1). The large samples have values similar to that of nearby Deccan basalt samples (Louzada et al., 2008) and other basalts and basaltic glasses (Pick and Tauxe, 1993).

The stable NRM characteristic of large samples is also observed for small samples chipped off these large samples: four subsamples with masses ranging from 0.006 to 0.058 g extracted from a 4.29-g parent irregular glass had similarly stable NRM during AF demagnetization, low MAD values, and high NRM/sIRM (Fig. 2F, Table S1). Therefore, the stable NRM of large glasses is a reflection of their fine spatial-scale NRM rather than of the aggregate sample. All of these data collectively indicate that while the large Lonar glasses have NRMs similar to typical terrestrial basalts, the small Lonar glasses have NRMs that are anomalously directionally unstable and inefficiently magnetized due a fundamental difference in fine-scale (much smaller than sample-scale) magnetization.

The NRM and rock magnetic properties of the small spherules in this study are extremely different from those measured by Misra et al. (2009) on millimeter and submillimeter diameter Lonar spherules. As discussed above, our several millimeter radius spherules had NRM/sIRM~0.2% on average. Our submillimeter spherules, which were extracted from the same outcrop as the spherules studied by Misra et al. (2009), had NRM per unit mass ≤~0.001 $Am^2\ kg^{-1}$ and NRM/sIRM ranging from 1.3 to 3.7×10^{-3}. In comparison, the submillimeter and millimeter spherules of Misra et al. (2009) had highly stable NRM (blocked to >130 mT) and exhibited curvilinear directional changes during AF demagnetization, NRM intensities ranging from 0.02 to 2 $Am^2\ kg^{-1}$, and NRM/sIRM ~1. The latter features are diagnostic of contamination by a strong IRM (like that from a hand magnet) and not of low-field TRM (see Section 2.7 of Weiss et al., 2010). Indeed, it was recently recognized that the spherules measured by Misra et al. (2009) had been previously separated from Lonar soils using a hand magnet with surface fields of ~140 mT (H. Newsom, personal communication).

4. Rock magnetic properties

In contrast to the great difference in NRM properties between small and large glasses, other than sIRM/mass (Fig. 4B) there is no obvious dependence of rock magnetic properties on sample mass indicative of domain state (Figs. 5–8). With one exception, all samples have ratios of sIRM to saturation magnetization, M_{rs}/M_s, and ratios of coercivity to coercivity of remanence, H_{cr}/H_c, consistent with fine grain sizes (mixture of pseudo single domain, single domain, and superparamagnetic crystals) as expected for glassy materials (Figs. 6 and 7). Lowrie–Fuller tests (Xu and Dunlop, 1995) for nearly all samples indicate low-field behavior (ARM more stable than IRM), consistent with pseudo single domain and smaller grain sizes (Fig. 5, Table S1). Also, there is also no dependence of coercivity, coercivity of remanence, mean destructive field (MDF) of IRM, MDF of ARM, or Cisowski R values with mass (Figs. 5 and 6, Table S1). All Lonar impact glasses have significantly higher MDF of ARM, MDF of IRM, and coercivities of remanence relative to the Lonar basalts (Louzada et al., 2008), presumably due to their relatively finer crystal sizes (Fig. 6). Small Lonar impact glasses have sIRM per unit mass considerably lower than Lonar basalts, while large Lonar impact glasses are comparable to the basalts (Fig. 4B). Submarine basaltic glasses have similarly weaker sIRM compared to the interior crystalline basalt pillow (Kent and Gee, 1996). By analogy with basaltic pillows, in which sIRM,

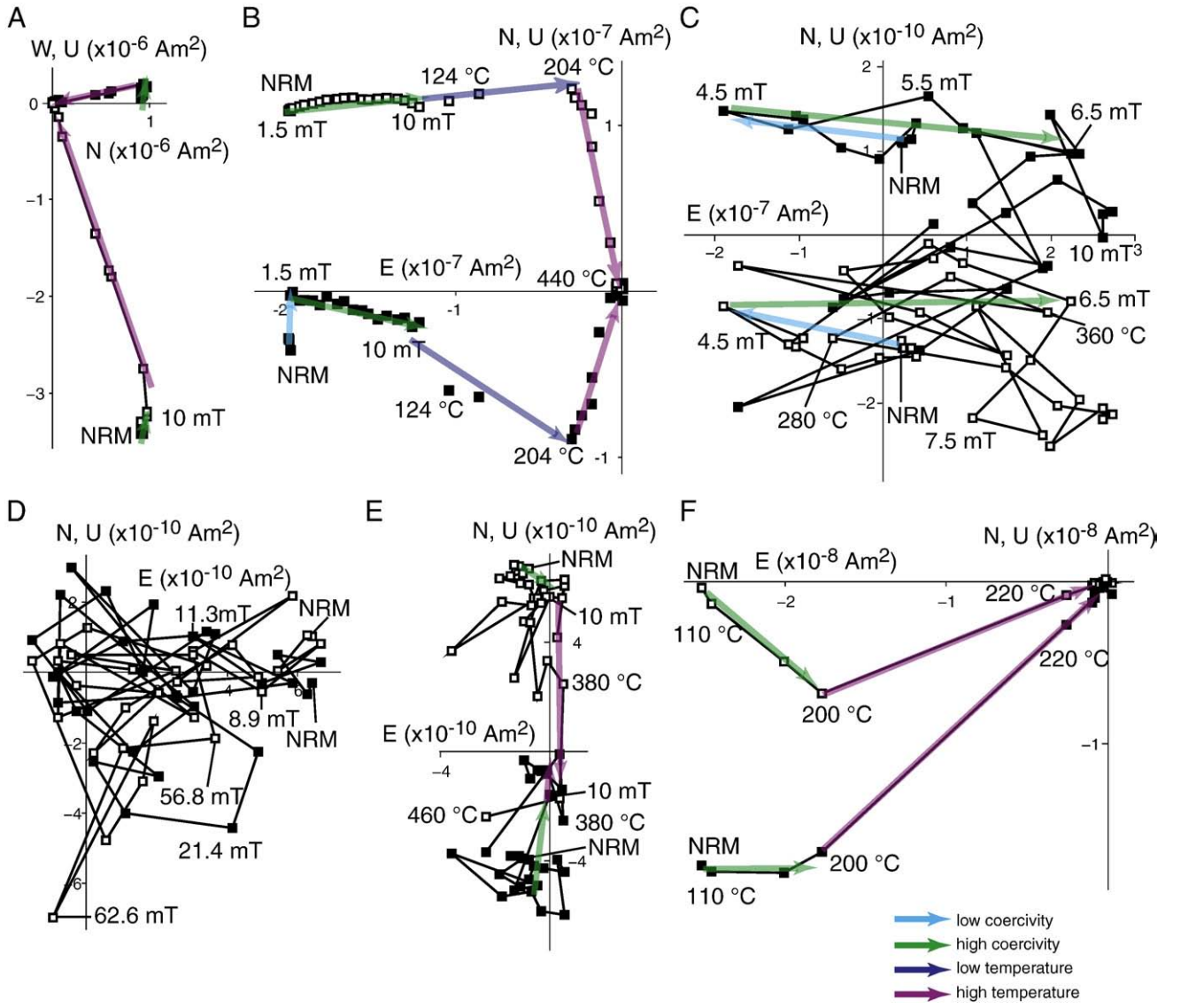

Fig. 2. NRM demagnetization behavior of Lonar glasses. Shown is the evolution of the endpoint of the NRM vector during AF and thermal demagnetization as projected onto arbitrary N–E and Z–E planes. Successive demagnetization steps are joined by straight black lines. (A) Large (2.17 g) irregular glass (LONGL-36) showing two stable components. (B) Large (0.78 g) irregular glass (LONGL-34) showing three main components. (C) Small (0.079 g) glass rod (LONGL-50) with poorly defined components. (D) Small (0.11 g) half-dumbbell (LONGL-5) showing no stable magnetization during AF demagnetization up to 83.9 mT. (E) Intermediate sized (0.26 g) glass ellipsoid (LONGL-19) with poorly defined components (highest temperature component is likely just spurious remanence acquired during thermal demagnetization). (F) Small chip off a large (4.29 g) irregular glass (LONGL-63) showing two stable components. For many samples, AF demagnetization to between 1.0 and 4.5 mT removes a very low-coercivity component (light blue). Subsequent AF demagnetization removes one or more higher coercivity components (green). Thermal demagnetization sometimes removes one or more low temperature components [dark purple (often in same direction as higher coercivity component (green)] followed by a high-temperature, usually origin-trending direction (dark purple). Small (~<0.8 g) glasses appear to have numerous high temperature components (points without superposed colored arrow).

saturation magnetization, susceptibility, and TRM increase with depth into the interior as a result of an increasing ratio of ferromagnetic crystals to glass (due to the decreasing cooling rate with depth) (Carlut and Kent, 2002; Marshall and Cox, 1971; Ryall and Ade-Hall, 1975), we suggest that this difference is due to the greater degree of crystallinity of the more slowly cooled, large samples. However, this analogy is not perfect because the magnetic recording properties of pillows like coercivity and M_{rs}/M_s also vary systematically with cooling rate in the pillow; this difference between pillows and Lonar glasses remains unexplained. In any case, a final, unambiguous indication of the general homogeneity of rock magnetic properties is that small glasses which have unstable NRMs during demagnetization acquire a strong (~10-100×NRM), single-component TRM after heating to 540 °C and cooling in a 50-μT (Earth-strength) laboratory field (Fig. 9).

Geochemical and petrographic analyses suggest that the main ferromagnetic mineral in Lonar glass is titanomagnetite $Fe_{3-x}Ti_xO_4$ with $x=0.1$–0.7 (Son and Koeberl, 2007). This result is consistent with S ratios (defined as the ratio of IRM after application of a 300-mT field to sIRM; Thomson and Oldfield, 1986) ranging between 0.95 and 1 (Fig. 6G, Table S1) and the observation that even the largest glass samples with stable NRMs become fully demagnetized at temperatures of 440–560 °C [which indicates $x=0.05$–0.2 following Dunlop and Ozdemir (1997) and assuming Ti as the main impurity]. Titanomagnetite of similar composition has been previously identified as a major remanence carrier in Lonar impact glasses (Misra et al., 2009) and basalts (Louzada et al., 2008) as well as most other Deccan basalts (Radhakrishnamurty and Subbarao, 1990).

5. Origin of magnetization

The great difference in NRM demagnetization behavior between small and large Lonar glasses could be explained by one of several

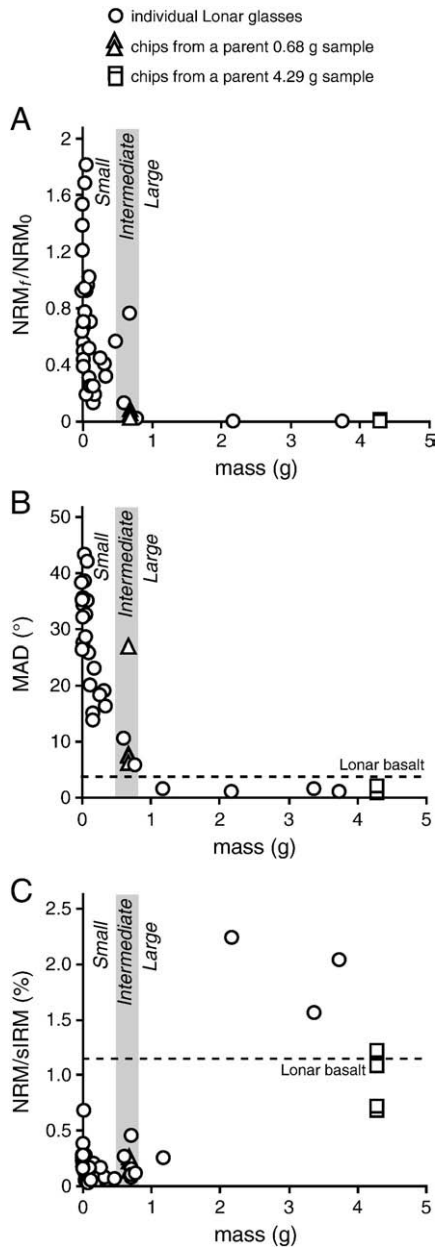

Fig. 3. NRM demagnetization behavior of Lonar impact glasses as a function of sample mass. (A) Ratio of final NRM intensity after laboratory demagnetization, NRM_f, to initial NRM, NRM_0. (B) MAD of least squares fits to high temperature or high coercivity NRM. Dashed line gives average values measured for 261 Lonar basalt cores by Louzada et al. (2008). (C) Ratio of NRM to sIRM. Dashed line gives average values measured for 20 Lonar basalt cores by Louzada et al. (2008). Splash form samples have masses to the left of the grey zone while irregularly-shaped samples have masses to the right of the grey zone. Samples with masses within grey zone have transitional shapes. Circles = individual glass samples unbroken in laboratory. Squares = subsamples broken from a single 4.29 g irregular glassy sample. Triangles = subsamples broken from a single 0.68-g glass sample.

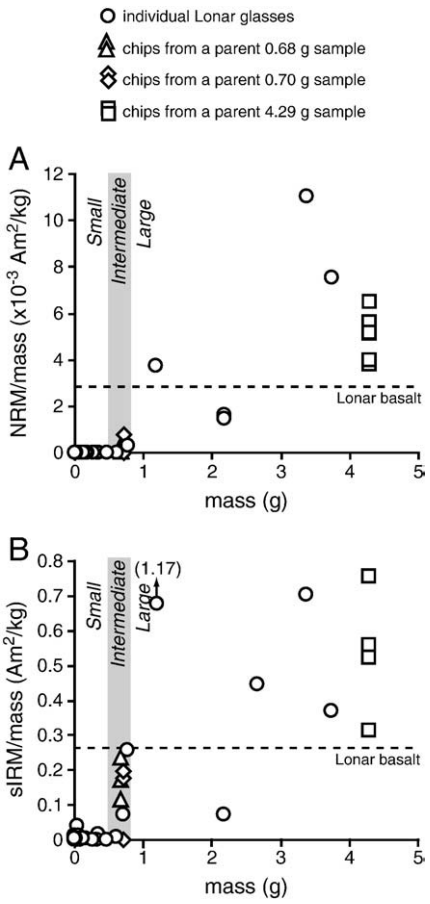

Fig. 4. (A) Mass-normalized NRM of Lonar impact glasses as a function of sample mass. (B) Mass-normalized sIRM of Lonar impact glasses as a function of sample mass. Splash form samples have masses to the left of the grey zone while irregularly-shaped samples have masses to the right of the grey zone. Samples with masses within grey zone have transitional shapes. Circles = individual glass samples unbroken in laboratory. Squares = subsamples broken from a single 4.29 g irregular glassy sample. Triangles = subsamples broken from a single 0.68-g glass sample. Diamonds: subsamples broken from a single 0.70-g glass sample. This figure does not include the five submillimeter glasses from the east rim because their masses were too small to measure accurately.

mechanisms. First, it is possible that this reflects a difference in rock magnetic properties between small and large glasses. In particular, the expected faster cooling time for small samples might have produced a greater fraction of low coercivity or low-blocking temperature crystals relative to those in large, slower cooled samples. This scenario might make the small spherules more susceptible to acquisition of overprints like viscous remanent magnetization or low-field IRM contamination from sample handling, and these overprints could form a complex multicomponent NRM as the spherules changed orientations in our laboratory or previously on the ground since the crater formed over the last 10^4–10^6 years (due to sedimentary processes). However, the lack of dependence of magnetic properties relevant for the fidelity of field recording (e.g., coercivity, H_{cr}/H_c, squareness, MDF, but not sIRM) on sample mass indicates that the difference in NRM demagnetization between small and large Lonar glasses is very unlikely to be due to differences in rock magnetic properties.

A second possible reason for the difference in NRM behaviors is that the smaller samples have fewer ferromagnetic crystals, which could lead to poorer fidelity magnetic properties via low resolution quantization of the recording process. Given that even some of the smaller (several mg) spherules that we analyzed should have at least millions of magnetite crystals (as indicated by sIRM values), theoretical calculations indicate that this hypothesis is highly unlikely in the absence of high bulk sample anisotropy (Brecher, 1976; Dickson, 1962; Irving et al., 1961; Kristjansson, 1973). In fact, our experiments suggest that nearly all samples have low remanence anisotropy and that this anisotropy has no mass-dependence. Although we have not measured formal anisotropy tensors for our samples, we found that small glasses acquire an sIRM and ARM (200 mT ac field, 2 mT dc bias field) with respective average inclinations of 86.8° ($1\sigma = 1.9°$, $N = 41$) and 87.5° ($1\sigma = 1.4°$, $N = 42$), while large glasses have ARM and sIRM average inclinations of 88.1° ($1\sigma = 0.6°$, $N = 9$) and 88.8° ($1\sigma = 0.7°$, $N = 9$). These

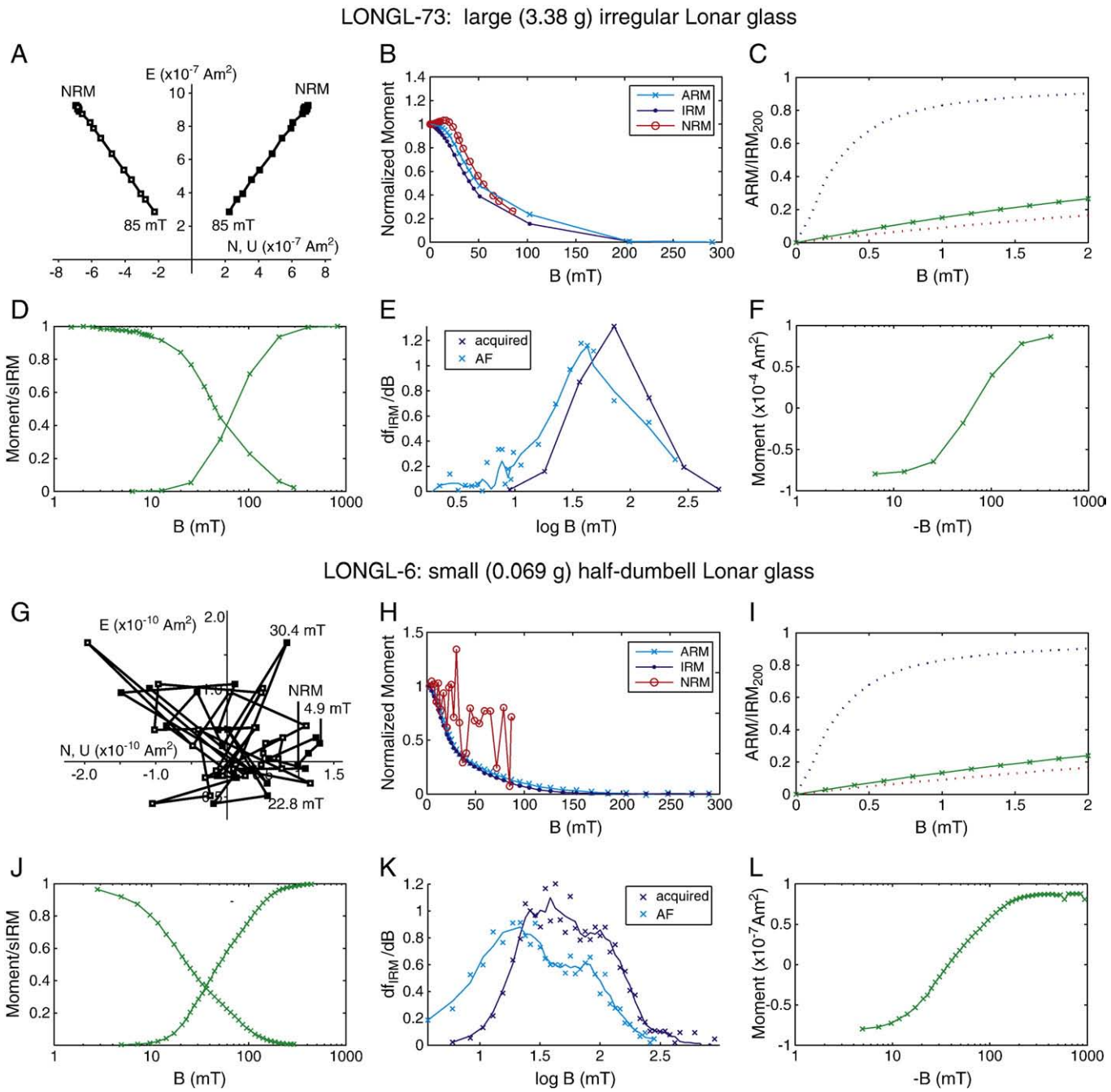

Fig. 5. NRM and detailed rock magnetic data for a characteristic large and small glass. These kinds of were data were used to compute the derived rock magnetic parameters shown in Figs. 3, 4, and 8. (A) AF demagnetization of NRM for large (3.38 g) irregular Lonar glass (LONGL-73). Shown is the evolution of the endpoint of the NRM vector during AF and thermal demagnetization as projected onto arbitrary N–E and Z–E planes. Successive demagnetization steps are joined by straight black lines. (B) Evolution of NRM intensity during AF demagnetization compared to that for ARM and IRM. ARM was acquired in a 200-mT peak AC field with 0.2-mT DC bias field (light blue symbols). IRM was acquired in a 200-mT field. Both curves are normalized to the starting value just prior to AF demagnetization. Comparison of the demagnetization rates for ARM and IRM constitutes the Lowrie–Fuller test (Lowrie and Fuller, 1971). (C) ARM acquisition experiments (Cisowski, 1981) on selected characteristic samples. Shown is the ARM acquired in a 200-mT AC field as a function of DC bias field. Lower dotted curve is that of highly interacting chiton tooth magnetite (Cisowski, 1981) and upper dotted curve is noninteracting magnetite in magnetotactic bacteria (Diaz Ricci et al., 1991). (D) IRM acquisition and AF demagnetization of IRM. Both curves are normalized to the highest-field IRM value. (E) Derivative of IRM acquisition (purple crosses) and AF demagnetization of IRM (light blue crosses). (F) Back-field DC demagnetization of sIRM. The intersection of this curve with zero magnetization specifies the coercivity of remanence. (G) AF demagnetization of NRM for small (0.069 g) half-dumbbell Lonar glass (LONGL-6). (H–L) Equivalent of curves (B–F) for LONGL-6.

inclinations are very close to the applied field inclination of ~85–90° (Fig. 8, Table S1). Most importantly, the previously described experiments in which small chips broken off large glasses were observed to have the same stable NRM demagnetization behavior as that of large unbroken samples strongly disfavors the small number of ferromagnetic crystals hypothesis.

A third hypothesis is that the small spherules are preferentially weathered due to their higher surface area to volume ratios. If this weathering produced ferromagnetic minerals as the samples changed orientation (due to sedimentary transport processes) on the ground and/or the absolute field direction changed, the samples could acquire a multicomponent crystallization remanent magnetization. However, nearly all spherules studied here had fresh, surfaces showing few signs of weathering and shiny, black, conchoidally fracturing interiors consistent with the presence of glass. Petrographic and geochemical studies of Lonar glasses confirm the general lack of interior

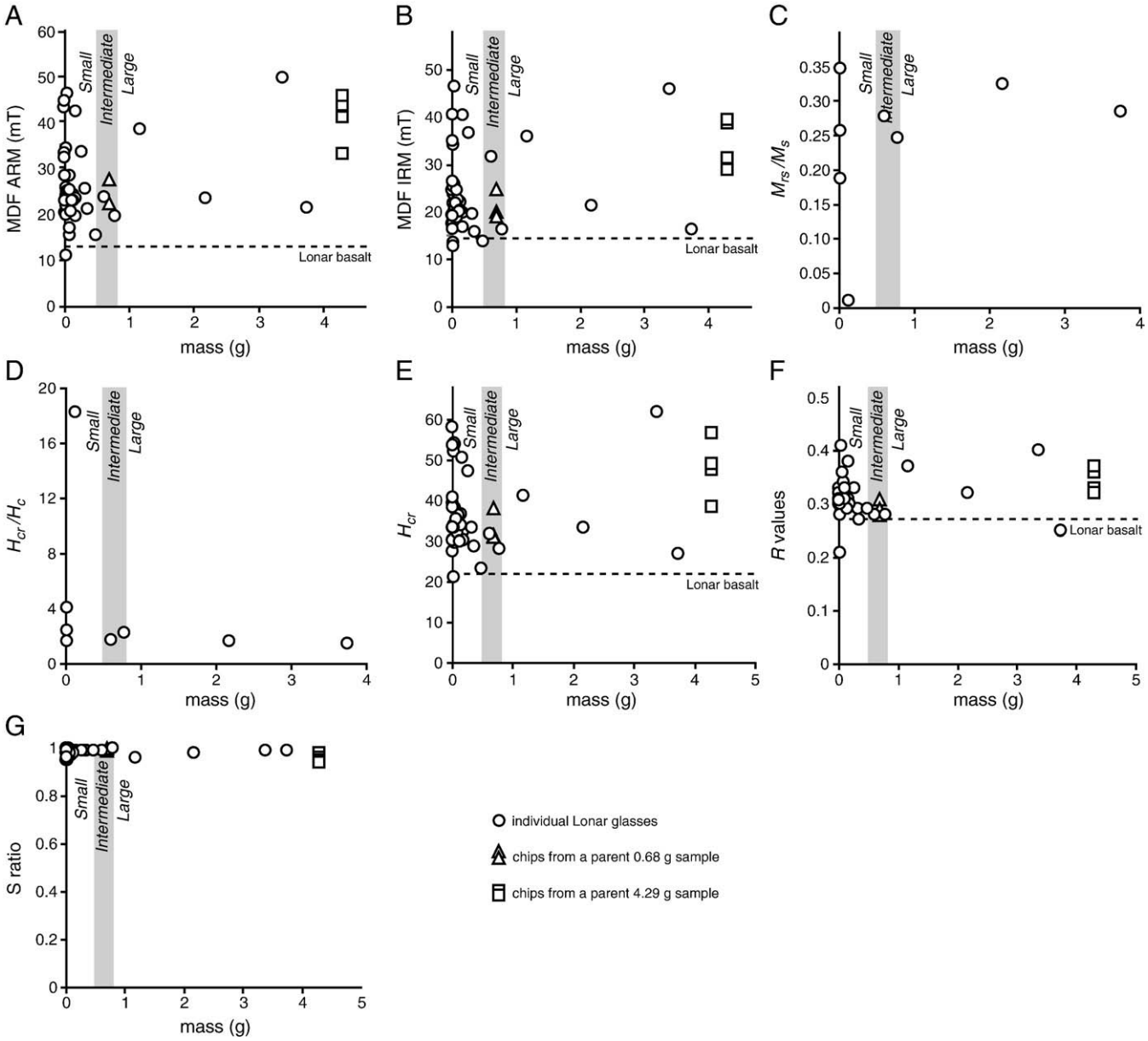

Fig. 6. Rock magnetic properties of Lonar impact glasses as a function of sample mass. (A) MDF of ARM. (B) MDF of IRM. (C) Ratio of sIRM to saturation magnetization. (D) Ratio of coercivity of remanence to coercivity versus sample mass. (E) Coercivity of remanence. (F) Cisowski *R* values. (G) S ratios (IRM from exposure to a 300-mT field divided by IRM from exposure to a 1-T field) for Lonar glasses. Dashed lines give average values measured for 20 Lonar basalt cores by Louzada et al. (2008). Splash form samples have masses less than grey zone while irregularly-shaped samples have masses greater than grey zone. Samples with masses within grey zone have transitional shapes. Circles = individual glass samples unbroken in laboratory. Squares = subsamples broken from a single 4.29-g irregular glassy sample. Triangles = subsamples broken from a single 0.68-g glass sample.

weathering products (Nayak, 1972; Fredriksson et al., 1973a; Fredriksson et al., 1973b; Sengupta, 1986; Murali et al., 1987; Osae et al., 2005; Ghosh and Day, 2009; Misra et al., 2009). Furthermore, the coercivity of remanence (Fig. 6E), S ratios (Fig. 6G), and the Curie points observed during thermal demagnetization of NRM of the glasses showing well-defined components (Fig. 2) are consistent with the dominance of titanomagnetite and general lack of significant quantities of goethite and hematite (see Dunlop and Ozdemir, 1997; Peters and Dekkers, 2003). We conclude that there is no evidence for remagnetization by weathering and therefore that weathering cannot account for the differences between the NRM of the large and small glasses.

A final hypothesis is that the difference in NRM between large and small glasses is a consequence of their difference in cooling times and, therefore, TRM acquisition times. If small (but not large) glasses cooled while in flight, during which their orientation changed rapidly with respect to the geomagnetic field (due to spin and translation), this would explain their distinctively highly multicomponent TRMs. Although non-translating but spinning glasses would be expected to acquire a single component NRM along the direction of their spin axes, the spin axes of flying glasses with curved trajectories should not acquire a stable NRM component because their spin axes would not be fixed with respect to the background field.

The viability of this explanation depends on the amount of time large and small spherules spent airborne versus that required to cool from the Curie point to ambient temperatures. During the first several seconds following a Lonar-sized impact, small particles will be entrained in the hot ejecta plume as it expands outward and will be well above the Curie temperature (Stöffler et al., 2002). When the plume disappears (as a result of expansion, cooling, condensation, and loss of incorporated particles), they will begin to cool and settle out of the atmosphere (N. Artemieva, personal communication). Assuming conductive cooling,

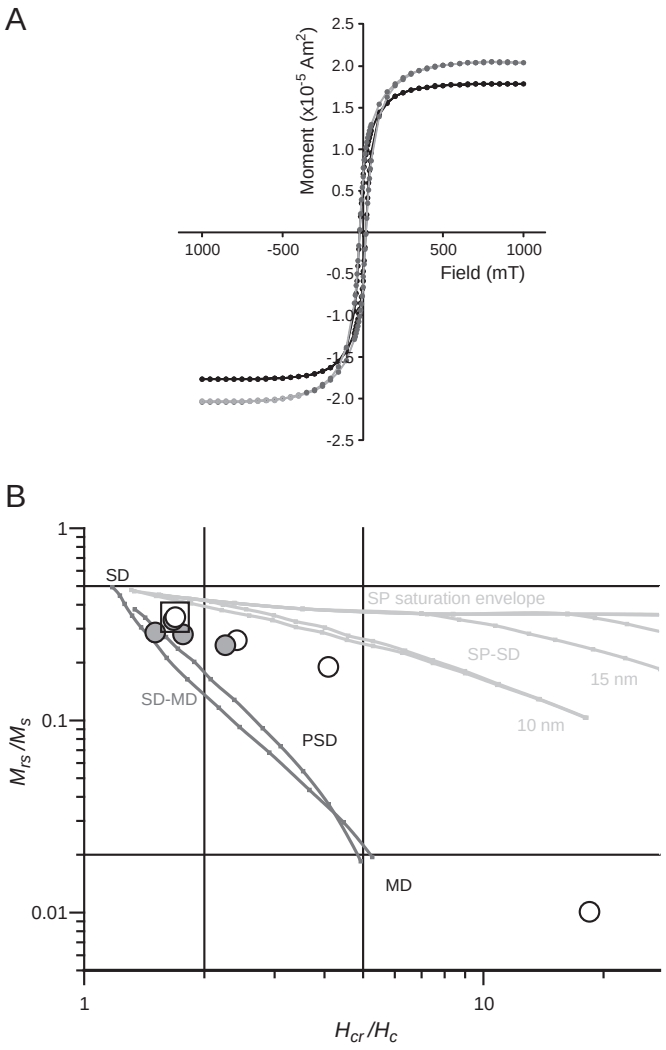

Fig. 7. Room temperature hysteresis data for Lonar glasses. (A) Hysteresis loops for large (2.17 g) irregular Lonar glass (LONGL-36) (grey curve) and small (0.018 g) Lonar glass (LONGL-52) (black curve). (B) Day plot (Day et al., 1977) showing the ratio of saturation remanence to saturation magnetization as a function of the ratio of coercivity of remanence to coercivity. Open circles=Large (N0.6 g) irregular glasses. Grey circles: small (b0.13 g) glasses. Single domain (SD)–multidomain (MD) and superparamagnetic (SP)–SD mixing lines (and associated SP grain sizes) of Dunlop (2002) are shown in grey. Hysteresis curves for the two boxed circles (open circle and red circle just beneath it) are shown in (A).

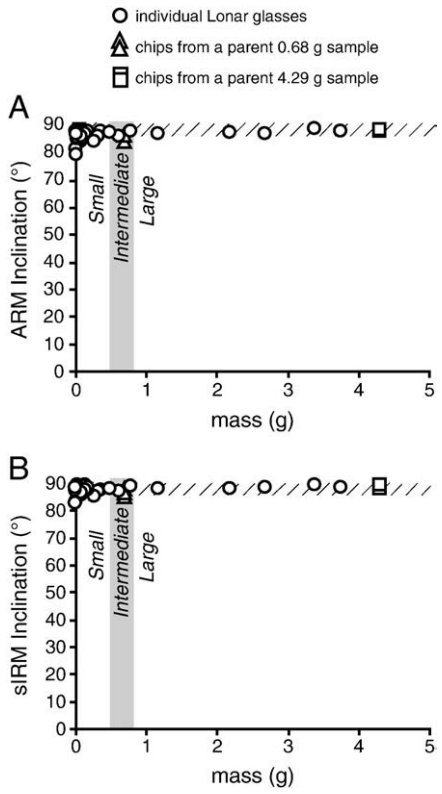

Fig. 8. (A) Inclination of ARM (200 mT peak ac field, 2 mT dc bias field). (B) Inclination of sIRM. Splash form samples have masses to the left of the grey zone while irregular-shaped samples have masses to the right of the grey zone. Inclination of field that produced ARM and sIRM was within range shown by hatched zone (within ≤5° of 90°).

which scales with the square of the sample radius, the millimeter radius, Lonar glasses are expected to cool from the Curie point to room temperature in several seconds, while centimeter radius glasses would take minutes to cool (using a thermal diffusivity typical of silicate rocks of 10^{-6} m^2 s^{-1}). These times are likely lower limits if the background atmosphere is still hot during settling. Numerical simulations suggest that submillimeter spherules are deposited as fallback over ~30 min, while centimeter-sized melts fallback in a couple of minutes (Artemieva, 2008). This is consistent with our simulations of the formation of a Lonar-sized crater, which indicate that it would take ~20 s from impact to lay down the near rim ejecta (see online Supplementary material); because all the spherules lie on top of the rim ejecta, they must have landed after that time. Therefore, small Lonar glasses should have cooled and magnetized while airborne, while large Lonar glasses should have cooled and magnetized after landing. This is remarkably consistent with our paleomagnetic data. Furthermore, the fact that none of the large glasses exhibit splash forms is also consistent with their having cooled below the Curie point after landing. We therefore strongly favor this hypothesis for the origin of weak, unstable in NRM in the small glasses: it is an inevitable consequence of motion of hot, moving rock cooling in a steady magnetic field.

6. Implications: motional magnetization and impact-generated fields

Nearly all natural samples carrying a TRM that have been previously studied using paleomagnetic techniques were essentially stationary during the time of original magnetization acquisition. As discussed above, probably the simplest interpretation of the unusual demagnetization behavior of the small Lonar glasses is that it is the result of progressive removal of different magnetization components that were blocked while the orientation of these spinning and translating samples changed relative to the paleomagnetic field. Such a motional magnetization process has, to our knowledge, never before been unambiguously identified in natural samples, with the possible exception of cosmic spherules (see below). Although it should be extremely rare on Earth, it may be one of the most frequent modes of remanence acquisition on the surfaces of small extraterrestrial bodies during the last several billion years.

There have been three previous paleomagnetic investigations of tektites, but none show evidence of motional NRM. Paleomagnetic studies of Muong Nuong-type layered tektites observed stable, generally single-component NRM (de Gasparis et al., 1975). This NRM stability is consistent with a leading model for the origin of these large tektites as solidified melt pools on the ground that were stationary during remanence acquisition (Wasson, 2003). Paleomagnetic studies of other very large (1–45 g) tektites and glassy impactites also observed apparently thermoremanent NRMs stable under AF (Guskova, 1980) and thermal demagnetization (Donofrio, 1977), with paleointensities of several tens of μT (Donofrio, 1977). These samples apparently also cooled through their Curie points

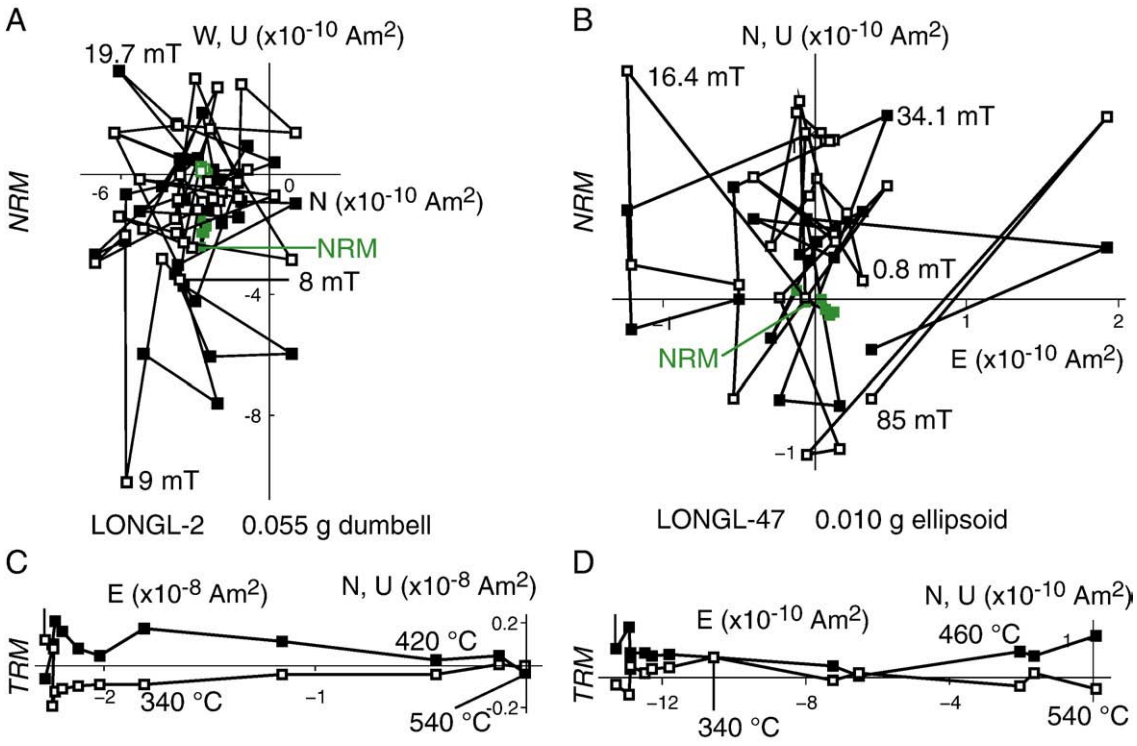

Fig. 9. Comparison of NRM and laboratory-induced TRM in several small, splash-form Lonar impact glasses. (A) Progressive AF demagnetization of NRM of 0.055-g dumbbell (LONGL-2) up to 290 mT. (B) Progressive AF demagnetization of NRM of 0.010-g ellipsoid (LONGL-47). The NRM directions in (A, B) are only directionally stable up to 3.0 mT (green symbols). (C) Progressive thermal demagnetization of sample shown in (A) up to 540 °C it had been heated to 540 °C in a 50-μT field oriented westward and horizontal. A single unidirectional magnetization nearly 100 times as intense as the NRM (C) is observed. (D) Progressive thermal demagnetization of sample shown in (B) up to 540 °C after it had been heated to 540 °C in a 50-μT field oriented westward and horizontal. A single unidirectional magnetization more than ten times as intense as the NRM is observed.

after landing, similar to the large Muong Nuong tektites and large Lonar glasses.

We are aware of three other classes of previously samples which might have acquired magnetization while in motion. Juvenile volcanic materials (e.g., pumice clasts), which should have cooled while airborne, might be expected to show scattered NRM behavior like that of Lonar glasses. However, essentially all previously studied pumice clasts have single component NRMs, apparently acquired after landing as a TRM or crystallization remanent magnetization during subsolidus alteration (Geissman, 1980; McClelland and Druitt, 1989; McClelland et al., 2004). Secondly, cosmic spherules should have acquired TRM while passing through the Earth's atmosphere. A recent study of 200- to 600-μm-diameter micrometeorite spherules collected from Antarctica (Suavet et al., 2009) observed single- or two-component NRM demagnetizing in a curvilinear fashion. The cooling time scales for these spherules from the Curie point to ambient temperatures, which are influenced by atmospheric heating, are estimated to be several seconds (Love and Brownlee, 1991). Although this is similar to our millimeter radius spherules, the coherent, curvilinear NRM of cosmic spherules (Suavet et al., 2009) indicates that unlike Lonar impact spherules, their orientation was only slowly changing with respect to the Earth's field during cooling.

Thirdly, individual chondrules and melted CAIs originally cooled over the temperature range ~1300–2000 °C/h at rates ranging from ~10 to 100 °C/h and from ~1 to 50 °C/h, respectively (Connolly et al., 2006). Extrapolating to ambient blackbody temperatures in the asteroid belt, this would indicate any TRM blocked during cooling would be acquired over hours to years. During this period, they were slowly orbiting the Sun (period of ~1.5 years for semimajor axis of 2 AU) while possibly entrained in more rapidly moving eddies and simultaneously spinning extremely rapidly (period of order 0.01 s; Miura et al., 2008; Tsuchiyama et al., 2003). In fact, chondrules and CAIs extracted from a variety meteorites tend to have stable NRM (Acton et al., 2007; Sugiura and Strangway, 1978, 1985; Wasilewski and Dickinson, 2000; Wasilewski and Saralker, 1981; Weiss et al., 2010). However, it is well known that many chondrules have been remagnetized by hand magnets (e.g., Wasilewski and Dickinson, 2000; Weiss et al., 2010), while many other chondrules were likely overprinted after accretion on the parent body (Nagata and Funaki, 1983; Sugiura and Strangway, 1985; Wasilewski and Saralker, 1981; Weiss et al., 2010). After removal of such an overprint on mutually oriented chondrules and CAIs from the Allende CV chondrite, the remaining remanence directions are highly scattered and do not demagnetize coherently. This remaining magnetization may be a motional NRM acquired before accretion of the parent body.

Our results also have important implications for the possibility of impact-generated fields at Lonar. The NRM/sIRM of all our Lonar glass samples are similar to (for large glasses) or ~2–40 times less than (for small glasses) the expected ~1% value for rocks carrying a thermo-remanent NRM acquired while stationary in the Earth's field. Therefore, there is no evidence of impact-generated paleofields substantially greater than several tens of μT at Lonar crater, consistent with our studies of Lonar Deccan Trap basalt flows (Louzada et al., 2008). Given the background geomagnetic field, any impact-generated fields weaker than ~50 μT would be difficult to detect from studies of Lonar and other terrestrial impact melts. Nevertheless, our upper limit on such fields is more than three orders of magnitude below the predictions of (Crawford and Schultz, 1999) described above. This is highly significant because our millimeter and smaller spherules are expected to have cooled quickly enough to acquire a stable magnetization via the transient field model of (Crawford and Schultz, 1999). Note that such a strong field would be recorded by even fast-moving samples because it would be blocked as a sIRM, which is acquired virtually instantaneously. On the other hand, Crawford and Schultz (1999) admit that their predicted field intensities are really extreme upper limits because the growth of

strong electric fields would be self-limited by discharging of dust grains in the plasma.

Finally, our results also have implications for the possibility of using impact glasses for paleointensity measurements. While the large glasses accurately recorded the paleointensity of the Earth's field at Lonar, paleointensities derived from the small glasses significantly underestimate its intensity, presumably due to the effects of rotation during cooling. Given the near complete lack of knowledge about the recent evolution of paleofields on extraterrestrial bodies, we expect that glassy impactites (in particular, relatively large, slowly cooled spherules and stationary melt sheets) will be extremely valuable paleointensity indicators.

Acknowledgements

We thank S. A. Soule and H. Newsom for assisting with field work, N. Artemieva for discussions about the thermal histories of impact spherules, two anonymous reviewers for helpful comments, and B. Carbone and K. Willis for administrative help. This work was supported by the NASA Mars Fundamental Research and Lunar Advanced Science and Exploration Research Programs, the NASA Lunar Science Institute, the Victor P. Starr Career Development Professorship, and the Harvard University Department of Earth Sciences.

Appendix A. Supplementary data

Supplementary data associated with this article can be found, in the online version, at doi:10.1016/j.epsl.2010.07.028.

References

Acton, G., Yin, Q.Z., Verosub, K.L., Jovane, L., Roth, A., Jacobsen, B., Ebel, D.S., 2007. Micromagnetic coercivity distributions and interactions in chondrules with implications for paleointensities of the early solar system. J. Geophys. Res. 112 10.1029/2006JB004655.

Artemieva, N.A., 2008. Tektites: model versus reality. Lunar Planet. Sci. 39 abstract #1651.

Brecher, A., 1976. Textural remanence: a new model of lunar rock magnetism. Earth Planet. Sci. Lett. 29, 131–145.

Carlut, J., Kent, D.V., 2002. Grain-size-dependent paleointensity results from very recent mid-oceanic ridge basalts. J. Geophys. Res. 107 10.1029/2001JB000439.

Chao, E.C.T., Boreman, J.A., Minkin, J.A., James, O.B., Desborough, G.A., 1970. Lunar glasses of impact origin: physical and chemical characteristics and geologic implications. J. Geophys. Res. 75, 7445–7479.

Cisowski, S., 1981. Interacting vs. non-interacting single-domain behavior in natural and synthetic samples. Phys. Earth Planet. Inter. 26, 56–62.

Connolly, H.C., Desch, S.J., Ash, R.D., Jones, R.H., 2006. Transient heating events in the protoplanetary nebula. In: Lauretta, D.S., McSween, H.Y. (Eds.), Meteorites and the Early Solar System II. University of Arizona Press, Tucson, pp. 383–397.

Crawford, D.A., Schultz, P.H., 1999. Electromagnetic properties of impact-generated plasma, vapor and debris. Int. J. Impact. Eng. 23, 169–180.

Culler, T.S., Becker, T.A., Muller, R.A., Renne, P.R., 2000. Lunar impact history from ^{40}Ar/^{39}Ar dating of glass spherules. Science 287, 1785–1788.

Day, R., Fuller, M., Schmidt, V.A., 1977. Hysteresis properties of titanomagnetites: grain-size and compositional dependence. Phys. Earth Planet. Inter. 13, 260–267.

de Gasparis, A.A., Cassidy, W.A., Fuller, M., 1975. Natural remanent magnetism of tektites of the Muong Nong type and its bearing on models of their origin. Geology 3, 605–607.

Diaz Ricci, J.C., Woodford, B.J., Kirschvink, J.L., Hoffman, M.R., 1991. Alteration of the magnetic properties of *Aquaspirillum magnetotacticum* by a pulse magnetization technique. Appl. Environ. Microbiol. 57, 3248–3254.

Dickson, G.O., 1962. The origin of small, randomly directed magnetic moments in demagnetized rocks. J. Geophys. Res. 67, 4943–4945.

Dressler, B.O., Reimold, W.U., 2001. Terrestrial impact melt rocks and glasses. Earth Sci. Rev. 56, 205–284.

Dunlop, D.J., Ozdemir, O., 1997. Rock Magnetism: Fundamentals and Frontiers. Cambridge University Press, New York. 573 pp.

Dunlop, D.J., 2002. Theory and application of the day plot (Mrs/Ms versus Hcr/Hc)—1. Theoretical curves and tests using titanomagnetite data. J. Geophys. Res. 107 10.1029/2001JB000486.

Elkins-Tanton, L.T., Aussillous, P., Bico, J., Quere, D., Bush, J.W.M., 2003. A laboratory model of splash-form tektites. Meteorit. Planet. Sci. 38, 1331–1340.

Fredriksson, K., Dube, A., Milton, D.J., Balasundaram, M.S., 1973a. Lonar Lake, India: an impact crater in basalt. Science 180, 862–864.

Fredriksson, K., Noonan, A., Nelen, J., 1973b. Meteoritic, lunar and Lonar impact chondrules. The Moon 7, 475–482.

Fuller, M., Cisowski, S.M., 1987. Lunar paleomagnetism. In: Jacobs, J.A. (Ed.), Geomagnetism 2. Academic Press, Orlando, pp. 307–455.

Gattacceca, J., Rochette, P., 2004. Toward a robust normalized magnetic paleointensity method applied to meteorites. Earth Planet. Sci. Lett. 227, 377–393.

Geissman, J.W., 1980. Paleomagnetism of ash-flow tuffs: microanalytical recognition of TRM components. J. Geophys. Res. 85, 1487–1499.

Ghosh, A., Day, R., 2009. Thermal simulation of a magma ocean on asteroid 4 Vesta. Lunar Planet. Sci. 40 abstract #1850.

Guskova, E.G., 1980. Magnetic properties of certain tektites. Meteoritika 39, 90–94.

Hartung, J.B., Hauser, E.E., Horz, F., Morrison, D.A., Schonfeld, E., Zook, H.A., et al., 1978. Lunar surface processes: report of the 12054 consortium. Proc. Lunar Planet. Sci. Conf. 9th, 2507–2537.

Irving, E., Stott, P.M., Ward, M.A., 1961. Demagnetization of igneous rocks by alternating magnetic fields. Phil. Mag. 6, 225–241.

Kent, D.V., Gee, J., 1996. Magnetic alteration of zero-age oceanic basalt. Geology 24, 703–706.

Kirschvink, J.L., 1980. The least-squares line and plane and the analysis of paleomagnetic data: examples from Siberia and Morocco. Geophys. J. R. Astr. Soc. 62, 699–718.

Kirschvink, J.L., Kopp, R.E., Raub, T.D., 2008. Rapid, precise, and high-sensitivity acquisition of paleomagnetic and rock-magnetic data: development of a low-noise automatic sample changing system for superconducting rock magnetometers. Geochem. Geophys. Geosyst. 9, Q05Y01 10.1029/2007GC001856.

Kletetschka, G., Acuna, M.H., Kohout, T., Wasilewski, P.J., Connerney, J.E.P., 2004. An empirical scaling law for acquisition of thermoremanent magnetization. Earth Planet. Sci. Lett. 226, 521–528.

Koeberl, C., 1986. Geochemistry of tektites and impact glasses. Annu. Rev. Earth Planet. Sci. 14, 323–350.

Kristjansson, L., 1973. The net magnetic moment of an assemblage of randomly oriented dipoles. Tellus 25, 300–304.

Levine, J., Becker, T.A., Muller, R.A., Renne, P.R., 2005. ^{40}Ar/^{39}Ar dating of Apollo 12 impact spherules. Geophys. Res. Lett. 32, L15201 10.1029/2005GL022874.

Louzada, K.L., Weiss, B.P., Maloof, A.C., Stewart, S.T., Swanson-Hysell, N., Soule, S.A., 2008. Paleomagnetism of Lonar impact crater. India. Earth Planet. Sci. Lett. 275, 309–319.

Love, S.G., Brownlee, D.E., 1991. Heating and thermal transformation of micrometeoroids entering the Earth's atmosphere. Icarus 89, 26–43.

Lowe, D.R., Byerly, G.R., 2010. Did LHB end not with a bang but a whimper? The geologic evidence. Lunar Planet. Sci. 41 abstract #2563.

Lowrie, W., Fuller, M., 1971. On the alternating-field demagnetization characteristics of multidomain thermoremanent magnetization in magnetite. J. Geophys. Res. 76, 6339–6349.

Maloof, A.C., Stewart, S.T., Weiss, B.P., Soule, S.A., Swanson-Hysell, N.L., Louzada, K.L., et al., 2010. Geology of Lonar Crater. India. Geol. Soc. Am. Bull. 122, 109–126.

Marshall, M., Cox, A., 1971. Magnetism of pillow basalts and their petrology. Geol. Soc. Am. Bull. 82, 537–552.

McClelland, E., Wilson, C.J.N., Bardot, L., 2004. Palaeotemperature determinations for the 1.8-ka Taupo ignimbrite, New Zealand, and implications for the emplacement history of a high-velocity pyroclastic flow. Bull. Volcanol. 66, 492–513.

McClelland, E.A., Druitt, T.H., 1989. Palaeomagnetic estimates of emplacement temperatures of pyroclastic deposits on Santorini. Greece. Bull. Volcanol. 51, 16–27.

Misra, S., Newsom, H.E., Prasad, M.S., Geissman, J.W., Dube, A., Sengupta, D., 2009. Geochemical identification of impactor for Lonar crater. India. Meteorit. Planet. Sci. 7, 1001–1018.

Miura, H., Nakamoto, T., Doi, M., 2008. Origin of three-dimensional shapes of chondrules: I. Hydrodynamics simulations of rotating droplet exposed to high-velocity rarefied gas flow. Icarus 197, 269–281.

Murali, A.V., Zolensky, M.E., Blanchard, D.P., 1987. Tektite-like bodies at Lonar Crater, India: implications for the origin of tektites. Proc. Lunar Planet. Sci. Conf. 17th, E729–E735.

Nagata, T., Funaki, M., 1983. Paleointensity of the Allende carbonaceous chondrite. Mem. Natl. Inst. Polar Res. Spec. Issue 30, 403–434.

Nayak, V.K., 1972. Glassy objects (impactite glasses?); a possible new evidence for meteoritic origin of the Lonar Crater, Maharashtra State. India. Earth Planet. Sci. Lett. 14, 1–6.

Osae, S., Misra, S., Koeberl, C., Sengupta, D., Ghosh, S., 2005. Target rocks, impact glasses, and melt rocks from the Lonar impact crater, India: petrography and geochemistry. Meteorit. Planet. Sci. 40, 1473–1492.

Peters, C., Dekkers, M.J., 2003. Selected room temperature magnetic parameters as a function of mineralogy, concentration and grain size. Phys. Chem. Earth 28, 659–667.

Pick, T., Tauxe, L., 1993. Holocene paleointensities: Thellier experiments on submarine basaltic glass from the East Pacific Rise. J. Geophys. Res. 98, 17949–17964.

Pullaiah, G., Irving, G., Buchan, K.L., Dunlop, D.J., 1975. Magnetization changes caused by burial and uplift. Earth Planet. Sci. Lett. 28, 133–143.

Radhakrishnamurty, C., Subbarao, K.V., 1990. Palaeomagnetism and rock magnetism of the Deccan traps. Proc. Indian Acad. Sci. 99, 669–680.

Rubin, A.M., 1985. Impact melt products of chondritic material. Rev. Geophys. 23, 277–300.

Ryall, P.J.C., Ade-Hall, J.M., 1975. Radial variation of magnetic properties in submarine pillow basalt. Can J. Earth Sci. 12, 1959–1969.

Simonson, B., Glass, B.P., 2004. Spherule layers—records of ancient impacts. Annu. Rev. Earth Planet. Sci. 32, 329–361.

Son, T.H., Koeberl, C., 2007. Chemical variation in Lonar impact glasses and impactites. GFF 129, 161–176.

Stöffler, D., Artemieva, N.A., Pierazzo, E., 2002. Modeling the Ries–Steinheim impact event and the formation of the moldavite strewn field. Meteorit. Planet. Sci. 37, 1893–1907.

Suavet, C., Gattacceca, J., Rochette, P., Perchiazzi, N., Folco, L., Duprat, J., Harvey, R.P., 2009. Magnetic properties of micrometeorites. J. Geophys. Res. 114, B04102 10.1029/2008JB005831.
Sugiura, N., Strangway, D.W., 1978. Magnetic studies of the Allende meteorite. LPI Conference 115.
Sugiura, N., Strangway, D.W., 1985. NRM directions around a centimeter-sized dark inclusion in Allende. Proc. Lunar Planet. Sci. Conf. 15th, C729–C738.
Thomson, R., Oldfield, F., 1986. Environmental Magnetism. Allen and Unwin, Concord. 227 pp.
Tsuchiyama, A., Shigeyoshi, R., Kawabata, T., Nakano, T., Uesugi, K., Shirono, S., 2003. Three-dimensional structures of chondrules and their high-speed rotation. Lunar Planet. Sci. 34 abstract #1271.
Warren, P.H., 2008. Lunar rock-rain: diverse silicate impact-vapor condensates in an Apollo-14 regolith breccia. Geochim. Cosmochim. Acta 72, 3562–3585.
Wasilewski, P., Dickinson, T., 2000. Aspects of the validation of magnetic remanence in meteorites. Meteorit. Planet. Sci. 35, 537–544.
Wasilewski, P.J., Saralker, C., 1981. Stable NRM and mineralogy in Allende: chondrules. Proc. Lunar Planet. Sci. Conf. 12th, 1217–1227.
Wasson, J.T., 2003. Large aerial bursts: an important class of terrestrial accretionary events. Astrobiology 3, 163–179.
Weiss, B.P., Gattacceca, J., Stanley, S., Rochette, P., Christensen, U.R., 2010. Paleomagnetic records of meteorites and early planetesimal differentiation. Space Sci. Rev. 152, 341–390.
Xu, S., Dunlop, D.J., 1995. Toward a better understanding of the Lowrie–Fuller test. J. Geophys. Res. 100, 22533–22542.
Yu, Y.J., 2006. How accurately can NRM/SIRM determine the ancient planetary magnetic field intensity? Earth Planet. Sci. Lett. 250, 27–37.
Zellner, N.E.B., Delano, J.W., Swindle, T.D., Barra, F., Olsen, E., Whittet, D.C.B., 2009a. Evidence from 40Ar/39Ar ages of lunar impact glasses for an increase in the impact rate 800 Ma ago. Geochim. Cosmochim. Acta 73, 4590–4597.
Zellner, N.E.B., Delano, J.W., Swindle, T.D., Barra, F., Olsen, E., Whittet, D.C.B., 2009b. Apollo 17 regolith, 71501, 262: a record of impact events and mare volcanism in lunar glasses. Meteorit. Planet. Sci. 44, 839–851.

Weiss, B. P. et al. (2010) Paleomagnetism of impact spherules from Lonar Crater, India and a test for impact-generated fields, *Earth Planet. Sci. Lett.*

Captions for Supplementary Material

Table S1. Supplementary Excel file containing the remanence and hysteresis measurements of Lonar spherules and impactites measured for this study. The columns contain the following information: A) Sample name, B) Mass of parent sample, C) Mass of sample [values equal those in (B) for all spherules which were not broken in the laboratory], D) brief description of sample E) Lists whether AF demagnetization was conducted and field of highest AF step, F) Lists whether thermal demagnetization was conducted and temperature of highest thermal demagnetization step, G) MAD of least squares fit to best-defined component, H) ratio of NRM after demagnetization to initial NRM, NRM_f/NRM_0, I) NRM magnitude, J) NRM per unit parent mass, K) sIRM as measured with 2G Superconducting Rock Magnetometer, L) sIRM per unit parent mass, M) NRM/sIRM, N) S ratio, O) MDF of an IRM acquired in a 200 mT dc field, P) MDF of an ARM acquired in an ac field of 200 mT and a dc field of 2 mT, Q) Results of Lowrie-Fuller test (ARM > IRM means ARM is more stable than IRM, IRM > ARM means IRM is more stable than ARM, ARM = IRM means ARM and IRM are similarly stable), R) Angle of moment after application of an ARM acquired in an ac field of 200 mT and a dc field of 2 mT (approximate orientation 85-90°), S) Angle of moment after application of an sIRM (approximate orientation 85-90°), T) Coercivity of remanence, U) Cisowski *R* value, V) sIRM as measured with vibrating sample magnetometer, W) saturation magnetization, X) Coercivity, Y) Ratio of saturation remanence to sIRM, Z) Ratio of coercivity of remanence to coercivity.

Movie S1. Calculations of ballistic ejecta for Lonar crater. The timescale for ballistic ejecta formation was determined from numerical simulations of a Lonar size impact event using the shock physics code CTH [1]. Movie S1 presents an example two-dimensional calculation of a 70-m diameter basalt bolide impacting a basalt half space at 20 km/s (from [2]). Although the exact impact conditions are unknown, the ejecta formation time scales with the size of the final crater. Materials were modeled using the quasi-static rheological model for basalt from Senft and Stewart [3] and the CTH SESAME tabular equation of state for basalt (a density-scaled version of the SiO_2 equation of state by Kerley [4]).

References

[1] J.M. McGlaun, S.L. Thompson, M.G. Elrick, CTH: A 3-dimensional shock-wave physics code, Int. J. Impact. Eng. 10(1990) 351-360.

[2] K.L. Louzada, B.P. Weiss, A.C. Maloof, S.T. Stewart, N. Swanson-Hysell, S.A. Soule, Paleomagnetism of Lonar impact crater, India, Earth Planet. Sci. Lett. 275(2008) 309-319.

[3] L.E. Senft, S.T. Stewart, Modeling impact cratering into layered surfaces, J. Geophys. Res. 112(2007) E11002.
[4] G. Kerley, Equations of State for Composite Materials, Kerley Publishing Services, Albuquerque, NM, 1999.